Inorganic Chemistry
Article
pubs.acs.org/IC

Heterobi- and Trimetallic Cerium(IV) *tert*-Butoxides with Mono-, Di-, and Trivalent Metals (*M* = K(I), Ge(II), Sn(II), Pb(II), Al(III), Fe(III))

Johannes Schläfer, Stefan Stucky, Wieland Tyrra, and Sanjay Mathur*

Institute of Inorganic Chemistry, University of Cologne, Greinstraße 6, D-50939 Cologne, Germany

Supporting Information

ABSTRACT: The reaction of Cerium Ammonium Nitrate (CAN) with varying amounts of KO^{t}Bu produced homometallic $Ce(O^tBu)_4(NC_5H_5)_2$ (**1**) and the heterometallic derivative $KCe_2(O^tBu)_{10}$ (**3**) characterized by X-ray diffraction and NMR spectroscopy. The oxo-alkoxide cluster $Ce_3O(O^tBu)_9$ (**2**) was obtained from a solution of cerium(IV) tetrakis(*tert*-butoxide) in *n*-heptane under stringent precautions to avoid any adventitious hydrolysis. Lewis acid-base reactions of in situ generated $Ce(O^tBu)_4(THF)_2$ (THF = tetrahydrofuran) with bi- and trivalent metal alkoxides $[M(O^tBu)_x]_n$ (M = Ge, Sn; x = 2; n = 2; M = Pb, x = 2; n = 3; M = Al, Fe; x = 3; n = 2) resulted in volatile products of the general formula $MCe(O^tBu)_{4+x}$ (M = Al (**4**), Fe (**5**); x = 3; M = Ge (**8**), Sn (**9**), Pb (**10**); x = 2) in high yields. By dissolving **4** and **5** in pyridine the solvent adducts $MCe(O^tBu)_7(NC_5H_5)$ (M = Al (**6**), Fe (**7**)) were formed, whereas **8** and **9** reacted with $Mo(CO)_6$ in boiling toluene to yield the termetallic complexes $(CO)_5MoM(\mu_2\text{-}O^tBu)_3Ce(O^tBu)_3$ (M = Ge (**11**), Sn (**12**)). The new compounds were characterized by comprehensive spectral studies, mass spectroscopy, and single crystal X-ray diffraction analysis.

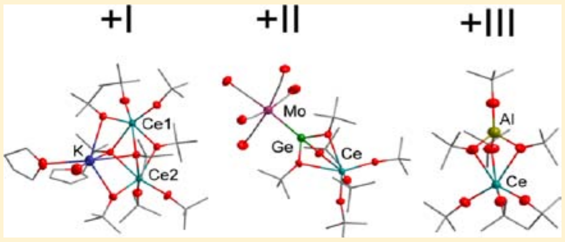

INTRODUCTION

Ceria (CeO_2) and its solid-solutions represent a class of outstanding functional ceramic materials because of their unique redox properties and oxygen storage capacity, which can be augmented in nanostructured phases.[1,2] With respect to soft chemical processing of advanced oxide ceramics, metal alkoxides are preferred starting materials because of preorganized metal−oxygen bonds in the precursor molecules and their intrinsic reactivity against nucleophilic attack (e.g., OH^-) as well as thermally labile nature of the organic periphery that makes them interesting precursors in sol−gel and chemical vapor deposition processes, respectively.[3] The preorganization of cations in heterobi- and -trimetallic alkoxide derivatives make them potential single-source precursors to multicomponent oxides. Given the chemical connectivity and vicinity of metal centers, diffusion is not the primary driving force for the phase-formation and as a result nanocrystalline ceramics with a homogeneous morphology and phase purity can be obtained at temperatures significantly lower than those required for solid-state reactions.[4] Whereas large numbers of precursors are available for the chemical synthesis of oxide ceramics and composites, the deposition of multicomponent ceria-based ceramics is less-investigated especially because of the lack of suitable volatile heterometallic complexes that will ensure constant precursor feeding as well as a uniform decomposition and growth rate.[4]

Cerium(IV) alkoxides have been known for many years, but their accessibility was aggravated because of lack of convenient synthetic pathways[5] until a salt metathesis reaction starting from readily available Ceric Ammonium Nitrate, $(NH_4)_2[Ce(NO_3)_6]$ (CAN), and alkali metal alkoxides was reported by Gradeff et al.,[6] which was elegantly modified and optimized by Evans et al.[7] Among the structurally characterized Cerium alkoxides, $[Ce(OCMe_2{}^iPr)_4]_2$,[8] $Ce_2(O^iPr)_8(HO^iPr)_2$,[9] and the corresponding oxo-alkoxide $Ce_4(\mu_4\text{-}O)(\mu_3\text{-}O^iPr)_2(\mu_2\text{-}O^iPr)_4(O^iPr)_8$[10] are the prominent representatives. In addition, the heteroleptic derivatives $Ce(O^tBu)_2(NO_3)_2(HO^tBu)_2$,[7] $Ce_2(OC^tBu_3)_6(\mu_2\text{-}OC_6H_4O)$,[11] the mixed-valence species $Ce_3(\mu_3\text{-}O^tBu)_2(\mu_2\text{-}O^tBu)_3(O^tBu)_5(NO_3)$,[12] $Ce_3(\mu_3\text{-}O^tBu)_2(\mu_2\text{-}O^tBu)_3(O^tBu)_6$,[13] and $Ce_4O(O^iPr)_{13}(HO^iPr)$[14] together with some donor functionalized[15] and fluorinated[16] alkoxide derivatives have been recently reported. In contrast to the tetravalent group 4 metals and the actinides uranium(IV) and thorium(IV), heterometallic cerium(IV) alkoxides remain relatively less investigated. To the best of our knowledge, the only structurally characterized heterobimetallic cerium alkoxides are limited to $Sr_2Ce_2(O^iPr)_{12}(HO^iPr)_4$,[17] $(MeOC_2H_4OMe)_2Na_2Ce(O^tBu)_6$, and $NaCe_2(O^tBu)_9$,[7] whereas the heteroleptic alkoxides include $Ce_2Ti_2(\mu_3\text{-}O)_2(\mu,\eta^2\text{-}OC(CH_3)_2C(CH_3)_2O)_4(O^iPr)_4(HO^iPr)_2$ and $Ce_2Nb_2(\mu_3\text{-}O)_2(\mu,\eta^2\text{-}OC(CH_3)_2C(CH_3)_2O)_4(O^iPr)_6$[18] as well as $Ba_4Ce_2O(thd)(O^iPr)_{12}$[19] (thd = tetramethylheptane-3,5-dionato) and a series of Schiff base metal complexes.[20]

In light of the above, the aim of this work was to develop new heterometallic *tert*-butoxides of cerium(IV) based on Lewis acid−base interactions of constituent alkoxides.

Received: January 8, 2013
Published: March 12, 2013

RESULTS AND DISCUSSION

Synthesis. Cerium(IV) tetrakis(*tert*-butoxide) was synthesized via a salt metathesis reaction starting from Cerium Ammonium Nitrate (CAN) and potassium *tert*-butoxide (KO^tBu) (eq 1). Depending on the stoichiometric amount of the alkali metal alkoxide, it is possible to replace the nitrate ligand successively by alkoxide groups as described by Evans et al. in the reaction of CAN with sodium *tert*-butoxide.[7] The homometallic tetrahydrofuran (THF) adduct $Ce(O^tBu)_4(THF)_2$ can be isolated from the reaction of CAN with 6 equiv of KO^tBu (eq 1). The coordination of two additional solvent molecules is attributed to the tendency of Ce(IV) to achieve octahedral configuration as described by Evans et al.[7] The bonding strength of the coordinated solvent molecules to the cerium center is apparently weak, and they can be partially removed under dynamic vacuum. Similarly, the solution dynamics indicate the formation of dimeric complexes of the general formula $Ce_2(O^tBu)_8(THF)_x$ where $x = 1{-}2$, although this value could not be confirmed, but the assumption is reasonable when considering structurally similar complexes of tetravalent metals, for example, $Zr_2(O^tBu)_8(N{\equiv}C\text{-}Me)$[21] or $M_2(O^tBu)_8(HO^tBu)$ (M = Th,[22] U[23]). Further, the THF molecules can be replaced by stronger donors such as pyridine in a facile reaction by dissolving the cerium complex in pyridine. The 6-fold coordinated mononuclear complex $Ce(O^tBu)_4(py)_2$ (**1**) was obtained as a pale yellow powder.

$$(NH_4)_2Ce(NO_3)_6 + 6KO^tBu \xrightarrow{THF} Ce(O^tBu)_4(THF)_2 + 6KNO_3 + 2NH_3 + 2HO^tBu \tag{1}$$

$$2(NH_4)_2Ce(NO_3)_6 + 13KO^tBu \rightarrow KCe_2(O^tBu)_9 + 12KNO_3 + 4NH_3 + 4HO^tBu \tag{2}$$

The propensity of $Ce(O^tBu)_4(THF)_2$ to form the trimetallic (M_3) oxo-alkoxide $Ce_3O(O^tBu)_{10}$ (**2**) in non coordinating solvents has been described in the literature and is also known for other tetravalent and trivalent metal *tert*-butoxides.[7,22−26] However, the mechanism for the formation of the $M_3O(O^tBu)_{10}$ is subject to the experimental conditions and reaction procedures. Because of the rigorous exclusion of water, a partial hydrolysis is very unlikely, however the elimination of $(^tBu)_2O$ could also lead to oxo-bridges although the ether could not be detected by NMR spectroscopy.

The heterometallic potassium derivative $KCe_2(O^tBu)_9$ (**3**) was synthesized via the reaction of CAN with 6.5 equiv of KO^tBu (eq 2), in which the in situ formed $Ce(O^tBu)_4(THF)_2$ was reacted with excess KO^tBu to form **3**. Crystallization of **3** from THF produced the solvent adduct $(THF)_2KCe_2(O^tBu)_9$ (**3′**) as confirmed by X-ray single crystal diffraction analysis. NMR data and elemental analysis revealed that the solvent free complex is isolable after drying in vacuum, which is consistent with observations made for the isostructural compounds $KU_2(O^tBu)_9$,[27] $NaTh_2(O^tBu)_9$[22] and $NaCe_2(O^tBu)_9$.[7] Attempts to synthesize complexes of potassium and cerium with a stoichiometric ratio of 1:1 or 2:1 analogous to $K_2Zr_2(O^tBu)_{10}$[28] and $(THF)_2Na_2Ce(O^tBu)_6$[7] by reacting CAN with stoichiometric amounts of KO^tBu, respectively, resulted exclusively in the formation of $KCe_2(O^tBu)_9$ (**3**).

The reaction of the trivalent metal alkoxides $[M^{III}(O^tBu)_3]_2$ (M^{III} = Al, Fe) with cerium(IV) tetrakis(*tert*-butoxide) in THF yielded the bimetallic solvent adducts of general formula $M^{III}Ce(O^tBu)_7(THF)$ with a labile THF coordination. The donor-free complexes were purified by vacuum sublimation at 140−150 °C (10^{-2} mbar) to yield $M^{III}Ce(O^tBu)_7$ (M^{III} = Al (**4**), Fe (**5**)). Dissolving the complexes in pyridine afforded the adducts $M^{III}Ce(O^tBu)_7(py)$ (M^{III} = Al (**6**), Fe (**7**)) in nearly quantitative yields.

In analogy, bimetallic compounds $M^{II}Ce(O^tBu)_6$ (M^{II} = Ge (**8**), Sn (**9**), Pb (**10**)) were obtained from the homometallic alkoxides (eq 3). The products were purified by vacuum sublimation at 130−150 °C (10^{-2} mbar). In contrast to heterometallic compounds based on trivalent metals, no evidence for solvent adducts was found neither at room temperature nor after prolonged refluxing in pyridine possibly because of tridentate ligation of the $\{M^{II}(O^tBu)_3\}^-$ anion. The stability of those complexes is further emphasized by combining an oxidizing (Ce^{IV}) and reducing (Ge^{II}, Sn^{II}) ion in one molecule without observation of any redox process.

$$Ce(O^tBu)_4(THF)_2 + \frac{1}{n}[M(O^tBu)_x]_n \rightarrow MCe(O^tBu)_{4+x} + 2THF \tag{3}$$

$$M = Ge, Sn;\ n = 2;\ x = 2;\ M = Pb;\ n = 3;\ x = 2;\ M = Al, Fe;\ n = 2;\ x = 3$$

It has been shown that complexes of group 13 and 14 metals which exhibit a free ns^2 electron pair possess the ability to form metal−metal bonds in a Lewis acid−base reaction with metal carbonyls.[29] In this work, **8** and **9** were reacted with $Mo(CO)_6$ in boiling toluene to yield the termetallic complexes $(CO)_5MoM^{II}(\mu_2\text{-}O^tBu)_3Ce(O^tBu)_3$ (M^{II} = Ge (**11**), Sn (**12**)) according to Scheme 1, while the attempted reaction with the analogous **10** did not occur even upon prolonged reactions periods. The slow reaction kinetics implied that the lone electron pair mainly possessed s-orbital character as reported for zirconium derivatives.[30] Even the reaction with the “activated” THF complex $Mo(CO)_5(THF)$ did not show any increased reactivity. The complexes **11** and **12** could not be obtained in analytical purity, neither by crystallization due to similar solubility properties of the starting materials nor by sublimation due to the thermal instability of the metal carbonyls.

Scheme 1. Formation of the Termetallic Complexes $(CO)_5MoM^{II}(\mu_2\text{-}O^tBu)_3Ce(O^tBu)_3$ (M^{II} = Ge (11), Sn (12)) Starting from the Heterobimetallic Alkoxides $M^{II}Ce(O^tBu)_6$ and $Mo(CO)_6$

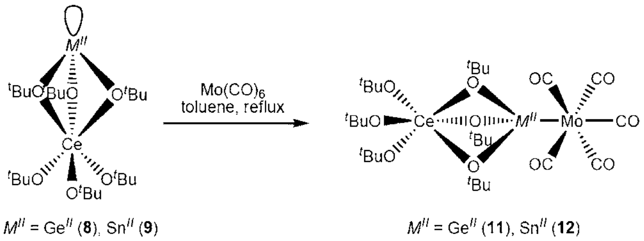

X-ray Diffraction Analysis. Crystals suitable for a single crystal X-ray diffraction study of $Ce(O^tBu)_4(py)_2$ (**1**) (Figure 1) were grown from a concentrated pyridine solution at −18 °C. It crystallizes in the triclinic space group $P\bar{1}$ with the cerium atom found in distorted octahedral coordination. The pyridine rings are oriented *cis* to each other because of the steric

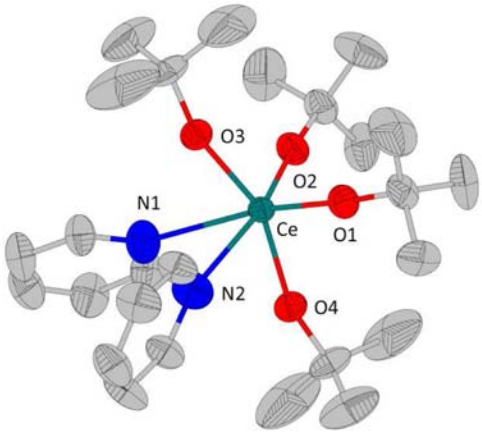

Figure 1. Molecular structure of $Ce(O^tBu)_4(py)_2$ (**1**). Thermal ellipsoids are shown at 50% probability level and the hydrogen atoms have been omitted for clarity. Selected bond lengths [Å] and angles [deg]: Ce−O(1) 2.090(5), Ce−O(2) 2.066(5), Ce−O(3) 2.115(4), Ce−O(4) 2.122(4), Ce−N(1) 2.691(5), Ce−N(2) 2.675(6); O(1)−Ce−O(2) 103.5(2), O(3)−Ce−N(2) 80.0(2), O(4)−Ce−N(1) 80.4(2), N(1)−Ce−N(2) 76.1(2).

bulkiness of the *tert*-butoxo groups causing a larger mean O−Ce−O angle of 98.2(2)° compared with the average N−Ce−O angle of 84.3(2)°. This assumption is further supported by smaller Ce−O−C angles of the alkoxide ligands in *cis* position (162.3(5)°) compared to those standing *trans* (173.9(5)°). Additionally, the *tert*-butoxo groups residing *trans* to each other exhibit a significantly shorter average bond length (2.078(5) Å) than that of those orientated *trans* to the pyridine ligands (2.119(4) Å). However, these deviations in bond angles and lengths can also emerge because of electronic effects. Similar observations were reported for $Th(O^tBu)_4(py)_2$.[22] The Ce−O bond lengths are in good agreement with those found for $Ce(O^tBu)_2(NO_3)_2(HO^tBu)_2$ and $(CH_3OC_2H_4OCH_3)_2Na_2Ce(O^tBu)_6$.[7]

The oxo-alkoxide cluster $Ce_3O(O^tBu)_{10}$ (**2**) (Figure 2) crystallized from a concentrated solution of $Ce(O^tBu)_4(THF)_2$ in *n*-heptane. The crystal structure revealed trigonal arrays of molecular units with a Ce−Ce distance of 3.527(1) Å. The molecular arrangement in the lattice showed hexagonal shaped channels propagating along the *c*-axis with a short diagonal length of d = 8.1 Å and an edge length of $x = d/\sqrt{3} = 4.6$ Å. Some residual electron density was found in the voids caused by strongly disordered intercalated *n*-heptane molecules. In the molecular core, metal centers are linked trough three μ_2-bridging *tert*-butoxo ligands to form a Ce_3-triangle capped by one tridentate *tert*-butoxo ligand and an oxo-group above and below the triangular plane. Each cerium atom binds additionally to two terminal *tert*-butoxo groups to complete the distorted octahedral geometry observed around each of the cerium atoms. The Ce−O bond lengths follow the trends reported earlier for oxo-alkoxides belonging to the M_3X_{11} class[24,25] with mean metal−oxygen distances of Ce−O 2.077(10) Å < μ_2-Ce-O 2.343(4) Å < μ_3-Ce-O 2.586(9) Å.

The bimetallic compound $(THF)_2KCe_2(O^tBu)_9$ (**3′**) (Figure 3) crystallized in the orthorhombic space group $Pc2_1b$ and displayed trigonal M_3 metal units known for other alkali metalates $KU_2(O^tBu)_9$,[27] $(THF)LiU_2(O^tBu)_9$,[31] $NaTh_2(O^tBu)_9$,[22] $NaCe_2(O^tBu)_9$,[7] and $(THF)_2KTi_2(O^iPr)_9$.[32] The trigonal metal unit is slightly distorted with a Ce−Ce distance of 3.6247(5) Å and a mean Ce−K distance of 3.758(2) Å. The complex showed significant differences in the metal−oxygen distances; whereas terminal *tert*-butoxo groups displayed slightly shorter mean Ce−O distances of 2.111(4) Å than the $\mu_{2(Ce-K)}$-bridging ligands (2.151(4) Å), the average Ce−O bond length of 2.395(4) Å for the $\mu_{2(Ce-Ce)}$-bridging alkoxo groups was comparable to the Ce−O distance of 2.425(4) Å for the μ_3-bridging ligands. Additionally, the mean K−O distance of the $\mu_{2(Ce-K)}$-bridging groups (2.922(6) Å) are

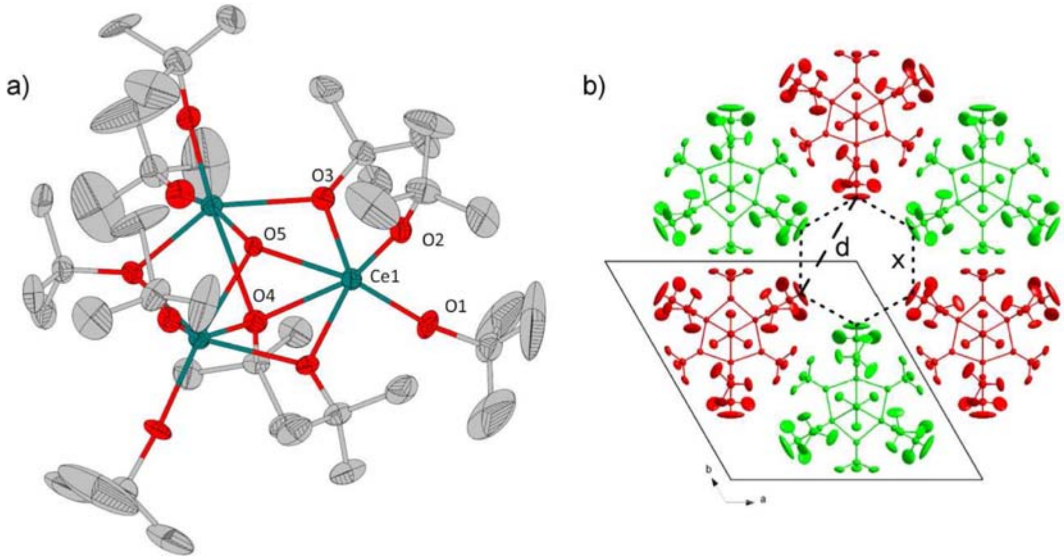

Figure 2. (a) Molecular structure of $Ce_3O(O^tBu)_{10}$ (**2**). Thermal ellipsoids are shown at 50% probability level, and the hydrogen atoms have been omitted for clarity. Selected bond lengths [Å] and angles [deg]: Ce−O(1) 2.110(8), Ce−O(2) 2.043(10), Ce−O(3) 2.343(4), Ce−O(4) 2.586(9), Ce−O(5) 2.248(6), Ce−Ce′ 3.527(1); O(1)−Ce−O(2) 100.6(4), O(3)−Ce−O(3)′ 141.5(2), O(4)−Ce−O(5) 63.1(5), Ce−O(3)−Ce′ 97.7(2); (b) Crystal packing diagram of **2**. View along *c*-axis. Molecules are colored according to the corresponding layer A and B (green: A (z); red: B ($z+1/2$)), d is the intermolecular distance C(12)−C(12) of two adjacent oxo-alkoxide clusters in one layer (short diagonal of the hexagon with an edge length of x).

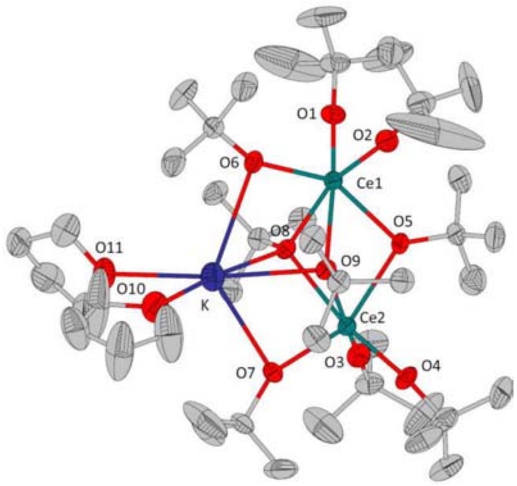

Figure 3. Molecular structure of $(THF)_2KCe_2(O^tBu)_9$ (**3′**). Thermal ellipsoids are shown at 50% probability level and the hydrogen atoms have been omitted for clarity. Selected bond lengths [Å]: Ce(1)−K 3.771(1), Ce(2)−K 3.744(2), Ce(1)−Ce(2) 3.6247(5), Ce(1)−O(1) 2.116(4), Ce(1)−O(2) 2.103(4), Ce(2)−O(3) 2.118(4), Ce(2)−O(4) 2.106(4), Ce(1)−O(5) 2.413(4), Ce(2)−O(5) 2.376(4), Ce(1)−O(6) 2.156(4), Ce(2)−O(7) 2.145(5), Ce(1)−O(8) 2.421(4), Ce(2)−O(8) 2.421(4), Ce(1)−O(9) 2.427(4), Ce(2)−O(9) 2.432(4), K−O(6) 2.946(5), K−O(7) 2.897(6), K−O(8) 2.748(4), K−O(9) 2.775(4), K−O(10) 2.779(6), K−O(11) 2.826(6).

elongated even exceeding the bond lengths to the THF ligands (2.803(6) Å) which is reported only for few complexes.[33] This supports further the ionogenic character of the complex and makes $KCe_2(O^tBu)_9$ an interesting synthon for transferring $\{Ce_2(O^tBu)_9\}^-$ anions on metal centers.

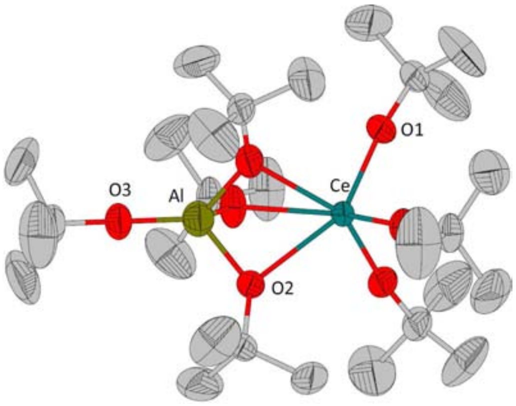

Figure 4. Molecular structure of $AlCe(O^tBu)_7$ (**4**). Thermal ellipsoids are shown at 50% probability level, and the hydrogen atoms have been omitted for clarity. Selected bond lengths [Å] and angles [deg]: Ce−Al 3.007(3), Ce−O(1) 2.073(4), Ce−O(2) 2.526(5), Al−O(2) 1.764(5), Al−O(3) 1.657(10), O(1)−Ce−O(1)′ 100.3(2), O(1)−Ce−O(2) 96.7(1), O(2)−Ce−O(2)′ 61.0(2), O(2)−Al-O(2)′ 93.2(2), O(2)−Al-O(3) 123.0(2).

The bimetallic complex $AlCe(O^tBu)_7$ (**4**) (Figure 4) crystallized in the chiral, trigonal space group $R3m$. The molecules show C_{3v} symmetry and are orientated along the crystallographic *c*-axis, with the metal centers and a terminal *tert*-butoxo ligand binding to aluminum being located on the crystallographic 3-fold axis encompassing a short Ce−Al contact (3.007(3) Å),[34] whereby the remaining ligands reside on mirror planes. The Ce−O bond lengths of 2.073(4) Å of the terminal ligands are in the expected range and the $\mu_{2(\mathrm{Ce-O})}$-bridging bonds show a remarkable elongation (2.526(5) Å) as observed for tetravalent metals in similar derivatives such as $SnZr(O^tBu)_6$ ($\mu_{2(\mathrm{Zr-O})}$ 2.309(8) Å).[35]

The crystal structures of **4** and **5** are isotypic. This is the first example of a $\{Fe(O^tBu)_4\}^-$ tetrahedral unit coordinating in a tridentate face bridging mode; a motif which has been postulated for the related $\{Al(O^tBu)_4\}^-$ tetrahedron however without any structural data.[36] All terminal Ce−O and all Fe−O distances were in the expected range.[37]

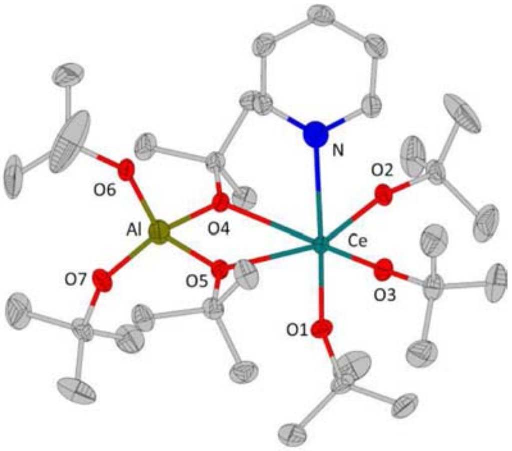

Figure 5. Molecular structure of $AlCe(O^tBu)_7(py)$ (**6**). Thermal ellipsoids are shown at 50% probability level, and the hydrogen atoms have been omitted for clarity. Selected bond lengths [Å] and angles [deg]: Ce−Al 3.4058(9), Ce−O(1) 2.065(2), Ce−O(2) 2.079(2), Ce−O(3) 2.088(2), Ce−O(4) 2.465(2), Ce−O(5) 2.460(2), Ce−N 2.689(3), Al−O(4) 1.796(2), Al−O(5) 1.788(2), Al−O(6) 1.714(2), Al−O(7) 1.693(2), O(1)−Ce−O(2) 96.50(9), O(1)−Ce−N 178.12(9), O(2)−Ce−O(3) 99.65(9), O(4)−Ce−O(5) 61.00(7), O(4)−Al-O(5) 88.4(1), O(6)−Al-O(7) 111.5(1).

The solvent adduct complex $AlCe(O^tBu)_7(py)$ (**6**) (Figure 5) and its isotypical analogue $FeCe(O^tBu)_7(py)$ (**7**) crystallized in the monoclinic space group $P2_1/c$. The molecular structure showed a less distorted (**6**: O−Al−O 109.1°; **7**: O−Fe−O 108.9°) tetrahedral arrangement of ligands when compared to **4** or **5**, respectively. The highly strained geometry as observed in **4** and **5** (**4**: O−Al−O 108.1°; **5**: O−Fe−O 107.6°) is apparently relaxed by the coordination of a neutral ligand on the cerium center resulting in the desired octahedral configuration.

The group 14 derivatives **8**−**10** crystallized in the hexagonal crystal system and showed a packing disorder along the M^{II}/Ce^{IV} vector caused by the head-to-tail superimposition of molecular structures as reported for the analogous zirconium derivatives.[35] Despite numerous attempts a structure solution of the diffraction data was impossible because of 180° disorder of the M^{II}/Ce vector. The unit cell showed three independent molecules whereby the metal centers are located on the 3-fold axis and the ligands on crystallographic mirror planes. For the tin derivative **9**, the metal−oxygen connectivity is depicted in Figure 6; however, a discussion of bonding parameters is not plausible because of the unrefined model.

The termetallic complex $(CO)_5MoGe(\mu_2\text{-}O^tBu)_3Ce(O^tBu)_3$ (**11**) (Figure 7) crystallized in the monoclinic space group $P2_1/c$. The molecules exhibit a linear arrangement (179.09(2)°) of

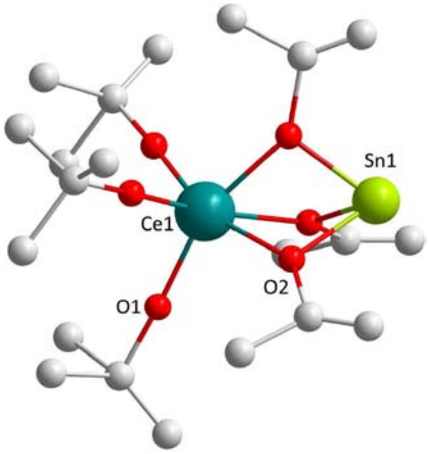

Figure 6. Ball and Stick representation of the molecular structure of $SnCe(O^tBu)_6$ (**9**). The hydrogen atoms and one methyl group could not be refined because of disorder.

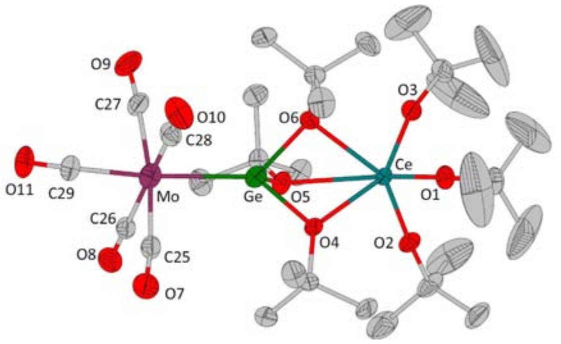

Figure 7. Molecular structure of $(CO)_5MoGe(\mu_2\text{-}O^tBu)_3Ce(O^tBu)_3$ (**11**). Thermal ellipsoids are shown at 50% probability level, and the hydrogen atoms have been omitted for clarity. Selected bond lengths [Å]: 11 Ce−Ge 3.2110(8), Mo−Ge 2.6518(7), Ce−O(1) 2.064(3), Ce−O(2) 2.049(3), Ce−O(3) 2.068(3), Ce−O(4) 2.488(3), Ce−O(5) 2.553(3), Ce−O(6) 2.512(3), Ge−O(4) 1.860(3), Ge−O(5) 1.855(3), Ge−O(6) 1.862(3), Mo−C(25) 2.043(5), Mo−C(26) 2.048(5), Mo−C(27) 2.032(5), Mo−C(28) 2.036(5), Mo−C(29) 1.992(5).

metal centers and an antiparallel interaction motif with C−O contact lengths between apical CO ligands of two adjacent molecules of 3.423(7) Å (Figure 8) which is below the required distance of <3.6 Å (sum of van der Waals radii plus 12%).[38] Although the molecular structure of **9** could not be successfully refined a shortening of the metal−metal and metal−oxygen distances can be assumed based on structures reported for similar complexes such as $SnTl(O^tBu)_3$ and $(CO)_5MoSn(\mu_2\text{-}O^tBu)_3Tl$.[39] The structure shows the comparable elongation of the Ce−O distance for the μ_2-bridging ligands caused by the Lewis acidity of the germanium center as already discussed for complexes **4** and **5**. The metal−metal bond length (2.6518(7) Å) matched with those of other Ge−Mo distances found in similar complexes.[29,40] Because of the weak π acceptor strength of germanium compared to carbon monoxide, a remarkable shortening of the *trans* standing Mo−C bond is noticeable (1.992(5) Å) because of a stronger back bonding of the molybdenum center.

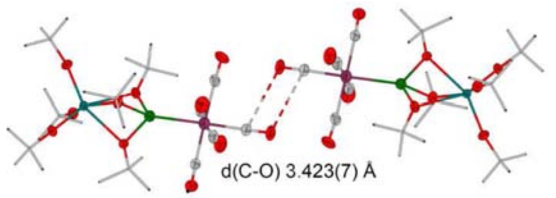

Figure 8. Crystal structure of $(CO)_5MoGe(\mu_2\text{-}O^tBu)_3Ce(O^tBu)_3$ (**11**). Formation of molecular dimers due to intermolecular electrostatic interactions of the *trans* standing carbonyl groups.

The heteroleptic complex $(CO)_5MoSn(\mu_2\text{-}O^tBu)_3Ce(O^tBu)_3$ (**12**) crystallized in the space group $P2_1/a$ with the similar structure motif as found for **11** with a Ce−Sn−Mo angle of 178.42(5)°. A short Ce−Sn distance of 3.367(2) Å is observable, and the Ce−O bond lengths of the bridging groups are elongated as in the germanium derivative (2.498(9) Å). The Sn−Mo bond causes a shortening of the *trans* standing Mo−C bond (1.99(2) Å) and showed no significant deviation from metal−metal bonds in comparable complexes.[29,39]

NMR Analysis. The homometallic pyridine complex **1** showed only one broad single resonance (1.61 ppm) for the *tert*-butoxo ligands and one set of resonances for the pyridine ligands in the ^1H NMR spectrum indicating a fluxional behavior at room temperature. In contrast, the polymetallic compound **2** displayed four sharp singlets in the ^1H NMR spectra at 1.44, 1.45, 1.92, and 1.95 ppm in an integrative ratio of 3:3:3:1 which correspond to two magnetically inequivalent terminal (2×3 O^tBu) and μ_2-(3 O^tBu) and μ_3-bridging (1 O^tBu) *tert*-butoxo groups, respectively. This finding demonstrates the rigidity of the M_3 core in solution. Similarly, the potassium derivative **3** showed four sharp singlets at 1.40, 1.63, 1.73, and 1.90 ppm in an integrative ratio of 2:4:2:1 assignable to the $\mu_{2(Ce-K)}$-, terminal, $\mu_{2(Ce-Ce)}$-, and the μ_3-bridging *tert*-butoxo groups, respectively.

The bimetallic aluminum complex **4** caused three resonances in the ^1H NMR spectrum for the bridging and the terminal ligands. The terminal *tert*-butoxo situated at the aluminum center and the bridging ligands produced two sharp singlets at 1.43 (1 O^tBu) and 1.57 ppm (3 O^tBu) whereas for the terminal alkoxo ligands situated at the cerium center only a broad signal at 1.44 ppm was detected. Contrary, the proton NMR spectrum of the pyridine adduct **6** shows only two broad resonances for the alkoxo groups with an integrative ratio of 3:4 which could be assigned to the terminal ligands bonding to the cerium center on one side and to the remaining bridging and terminal *tert*-butoxo groups on the other side. The ^{27}Al NMR spectra indicated a tetrahedral coordination sphere around the Al(III) centers. The chemical shifts for both compounds (**4**: 59 ppm, $w_{1/2} = 1400$ Hz; **6**: 47 ppm, $w_{1/2} = 1200$ Hz) fall in the typical range of AlO_4-tetrahedra.[41]

The complexes **8**−**10** exhibited two equally intense resonances in the ^1H NMR spectra for the bridging and terminal alkoxo groups. For the tin and lead derivative, the μ_2-bridging ligands could be assigned because of the coupling of the hetero nuclei with the methyl carbon atoms ($^3J(^{13}C,^{119}Sn) = 26$ Hz, $^3J(^{13}C,^{207}Pb) = 25$ Hz). The ^{119}Sn NMR spectrum of **9** showed only one single resonance at −249 ppm consistent with a divalent tin center in a pseudotetrahedral coordination sphere with three μ_2-bridging alkoxide groups.[35] The ^{207}Pb NMR spectra of **10** showed a resonance at a chemical shift of +1356 ppm, which is in agreement with NMR shifts reported for similar compounds such as $PbZr(O^tBu)_6$.[30] The ^1H NMR spectra of the Lewis acid−base adducts **11** and **12** differ in chemical shift compared to the bimetallic adducts. For the tin derivative the bridging alkoxo groups could be assigned because of a ^{1}H,^{119}Sn HMBC correlation experiment. The signal of the terminal ligands is shifted to higher field, and the resonance corresponding to the bridging groups is shifted to lower field. The carbonyl ligands exhibited two signals in the ^{13}C NMR spectrum in an integrative ratio of 4:1 for the equatorial ligands at 206.2 ppm and the axial ligand at 209.7 ppm for complex **12** and at 206.8 ppm and 210.0 ppm for complex **11**. The signal in the ^{119}Sn NMR spectrum was shifted significantly downfield to −16 ppm because of the decrease of electron density around the tin ion by coordinative bonding to molybdenum as it is also observed for other tin transition metal carbonyl compounds.[29] The complete NMR data are given in the Experimental Section.

Mass Spectrometric Investigations. Mass spectra recorded for the volatile complexes **4**, **5**, **8**−**10** confirmed their gas phase stability and monomeric nature. The most intense peak for all compounds is the fragment $[\text{M-OC}_4\text{H}_9]^+$ which is caused by the elimination of one *tert*-butoxo group. Further, peaks for the fragments $[\text{M-CH}_3]^+$, $[\text{M-2(OC}_4\text{H}_9)]^+$, and $[M\text{Ce(O}^t\text{Bu)}_{x+1}\text{O}]^+$ (M = Al, Fe; x = 3; M = Ge, Sn, Pb; x = 2) were observed, while the molecular ion peak was only detectable for the complexes **8** and **9**. No additional peaks with higher m/z ratios than $[\text{M}]^+$ were found proving the monomeric nature of the complexes in the gas phase.

Thermogravimetric Profiles. The decomposition behavior of the bimetallic complexes **4**, **5**, **8**−**10** under a constant nitrogen flow in sealed aluminum cartridges showed a sharp decomposition step in the range of 280−350 °C followed by a constant mass loss up to 630 °C (Figure 9). A gradual mass loss observed before the decomposition sets in is possibly caused by partial hydrolysis due to environmental moisture. The experimental weight loss is in good agreement with the calculated values which illustrated clean decomposition properties of the alkoxides with low carbon contamination. The oxidic products were assumed to have a composition of CeO_2-$0.5(M^{III}{}_2\text{O}_3)$ for **4**, **5** and CeO_2-$M^{II}\text{O}$ or CeO_2-$0.5(M^0/M^{IV}\text{O}_2)$ for **8**−**10**, respectively, which results in remaining weights for the decomposition products as follows: wt % (calcd/found): **4**, 0.33/0.34; **5**, 0.36/0.38; **8**, 0.40/0.44; **9**, 0.44/0.46, **10**: 0.50/0.52.

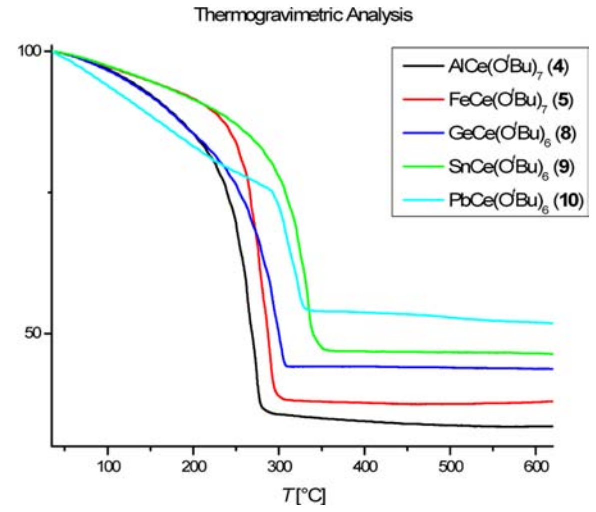

Figure 9. TGA profiles of the complexes **4**, **5**, **8**−**10** under nitrogen atmosphere with a heating rate of 5 °C/min.

CONCLUSIONS

The first structural characterization of monometallic complexes $\text{Ce(O}^t\text{Bu)}_4\text{(py)}_2$ (**1**) and $\text{Ce}_3\text{O(O}^t\text{Bu)}_{10}$ (**2**) was elucidated, and a general synthetic protocol for heterobimetallic cerium(IV) *tert*-butoxides was established. The Lewis acid−base reaction of in situ generated $\text{Ce(O}^t\text{Bu)}_4\text{(THF)}_2$ with the appropriate homometallic *tert*-butoxides produced polymetallic alkoxides of mono-, di-, and trivalent metal ions (**3**−**10**) in good yields. Thermogravimetric measurements indicate their single step decomposition and make them potential precursors for mixed-metal oxides and composites. $M^{III}\text{Ce(O}^t\text{Bu)}_7$ (M^{III} = Al, Fe) represent the first examples of heterometallic cerium(IV) alkoxides with trivalent group 13 and transition metal partners. The Lewis basicity of the ns^2 electron pair available on bivalent Sn and Ge was used to construct termetallic complexes $\text{(CO)}_5\text{Mo}M^{II}(\mu_2\text{-O}^t\text{Bu})_3\text{Ce(O}^t\text{Bu)}_3$ (M^{II} = Ge (**11**), Sn (**12**)) by the reaction of the corresponding heterobimetallic alkoxides **8** and **9** and Mo(CO)_6.

EXPERIMENTAL SECTION

Reagents and General Procedures. All manipulations were carried out under dinitrogen using Stock-type all-glass assemblies. The homometallic alkoxides $\text{Ce(O}^t\text{Bu)}_4\text{(THF)}_2$,[7] $[\text{Al(O}^t\text{Bu)}_3]_2$,[41] $[\text{Fe(O}^t\text{Bu)}_3]_2$,[37] $[\text{Ge(O}^t\text{Bu)}_2]_2$,[42] $[\text{Sn(O}^t\text{Bu)}_2]_2$,[43] and $[\text{Pb(O}^t\text{Bu)}_2]_3$[42] were synthesized according to literature methods. KO^{t}Bu and Mo(CO)_6 were obtained from Aldrich and purified by sublimation under reduced pressure. Cerium(IV) Ammonium Nitrate (CAN, Aldrich, 98,5%) was dried in dynamic vacuum at least for 7 h. All solvents were dried over sodium or CaH_2 respectively, and distilled prior to use. NMR spectra were recorded on a Bruker Avance II 300 spectrometer. ^{1}H NMR (300.1 MHz) and ^{13}C NMR (75.7 MHz) chemical shifts are reported in parts per million relative to external tetramethylsilane and are referenced internally to the proton impurity or ^{13}C signal of the solvent, respectively. Assignment of all ^{13}C NMR signals of the *tert*-butoxo groups was made on the basis of HMBC experiments. ^{119}Sn NMR (111.9 MHz) and ^{207}Pb NMR (62.8 MHz) chemical shifts are reported relative to $\text{Sn(CH}_3)_4$ and $\text{Pb(CH}_3)_4$ and are referenced externally to $\text{Sn(CH}_3)_4$ and $\text{Pb(NO}_3)_2/\text{D}_2\text{O}$; ^{27}Al NMR (78.2 MHz) is referenced externally to $[\text{Al(H}_2\text{O)}_6]\text{Cl}_3$. Mass spectra were recorded on a Finnigan MAT 95 (EI, 20 eV) in m/z (intensity in %). Elemental analyses were carried out on a HEKAtech CHNS Euro EA 3000. DTA measurements were preformed on a TGA/DSC1 (Mettler-Toledo GmbH, Gießen, Germany) apparatus. IR spectra were recorded on a Bruker IFS 66v/S spectrometer. The absorption bands are reported in cm^{-1} and were assigned as follows: weak (w), medium (m), strong (s), very strong (vs), and shoulder (sh). Data collection for X-ray structure elucidation (Tables 1 and 2) was performed on a STOE IPDS I/II/2T diffractometer using graphite-monochromated MoKα radiation (0.71071 Å). The programs used in this work are STOE's X-Area[44] and the WINGX suite of programs,[45] including SIR-92[46] and SHELXL-97[47] for structure solution and refinement. H-atoms were calculated geometrically, and a riding model was applied during the refinement process. In the crystal structure of **2** and **3** large or medium solvent accessible voids are present and also some remaining electron density could be found. It can be attributed to strongly disordered *n*-heptane or THF molecules, respectively, which could not be resolved properly. Compound **4** and **5** were solved in the acentric space group $R3m$ whereas in both cases the Flack parameter shows a remarkable deviation of 0 (**4**: 0.70(3); **5**: 0.29(4)). Despite careful analysis of the reflection data no additional symmetry was found and in course of this a twin refinement for a racemic crystal was carried out.

Synthesis of $\text{Ce(O}^t\text{Bu)}_4\text{(py)}_2$ (1). The product was obtained as a pale yellow powder in nearly quantitative yield (1.02 g, 96%) by dissolving 1.03 g (1.8 mmol) $\text{Ce(O}^t\text{Bu)}_4\text{(THF)}_2$ in dry pyridine. Crystals suitable for single crystal X-ray diffraction were grown from a concentrated pyridine solution at −18 °C. ^{1}H NMR (C_6D_6, 25 °C): δ

Table 1. Crystallographic Data for the Complexes 1−5

	1	2	3	4	5
formula	$CeC_{26}H_{46}N_2O_4$	$Ce_3C_{40}H_{90}O_{11}$	$Ce_2KC_{44}H_{97}O_{11}$	$CeAlC_{28}H_{63}O_7$	$CeFeC_{28}H_{63}O_7$
M_r /g mol^{-1}	590.77	1167.48	1121.56	678.88	707.75
cryst syst	triclinic	hexagonal	orthorhombic	trigonal	trigonal
space group	$P\bar{1}$	$P6_3mc$	$Pc2_1b$	$R3m$	$R3m$
T /K	293(2)	293(2)	170(2)	293(2)	293(2)
a /Å	9.843(1)	18.116(2)	17.0121(4)	15.775(5)	15.815(5)
b /Å	9.846(1)	18.116(2)	18.0594(4)	15.775(5)	15.815(5)
c /Å	16.783(2)	10.988(9)	19.6945(6)	13.208(5)	13.272(5)
α /deg	93.92(2)	90.00	90.00	90.00	90.00
β /deg	93.83(2)	90.00	90.00	90.00	90.00
γ /deg	100.91(2)	120.00	90.00	120.00	120.00
V /Å ^{3}	1588.1(4)	3123.3(2)	6050.7(3)	2846.5(17)	2874.8(17)
Z	2	2	4	3	3
μ (Mo-K_α) /mm^{-1}	1.46	2.188	1.598	1.256	1.584
no. of unique rflns, R_{int}	5255, 0.0877	2566, 0.0934	12814, 0.0930	1481, 0.0519	1594, 0.0535
goodness of fit	0.813	0.855	1.053	1.091	1.117
final R indices $[I > 2\sigma(I)]$: R_1, wR_2	0.0399, 0.0808	0.0345, 0.0895	0.0477, 0.1242	0.0339, 0.0835	0.0390, 0.0996
R indices (all data): R_1, wR_2	0.0777, 0.0905	0.0619, 0.0968	0.0566, 0.1318	0.0340, 0.0844	0.0397, 0.1004

Table 2. Crystallographic Data for the Complexes 6, 7, 11, 12

	6	7	11	12
formula	$CeAlC_{33}H_{68}NO_7$	$CeFeC_{33}H_{68}NO_7$	$CeGeMoC_{29}H_{54}O_{11}$	$CeSnMoC_{29}H_{54}O_{11}$
M_r /g mol^{-1}	757.98	786.85	887.37	933.47
cryst syst	monoclinic	monoclinic	monoclinic	monoclinic
space group	$P2_1/c$	$P2_1/c$	$P2_1/c$	$P2_1/a$
T /K	170(2)	293(2)	170(2)	293(2)
a /Å	12.6300(4)	13.063(1)	19.762(5)	20.530(4)
b /Å	24.4223(5)	24.867(2)	10.172(5)	10.2424(11)
c /Å	14.5476(5)	14.732(1)	20.194(5)	20.544(4)
α /deg	90.00	90.00	90.00	90.00
β /deg	114.786(2)	116.151(5)	103.300(5)	103.761(15)
γ /deg	90.00	90.00	90.00	90.00
V /Å^3	4073.9(2)	4295.7(6)	3951(2)	4196.0(12)
Z	4	4	4	4
μ (Mo-K_α) /mm^{-1}	1.178	1.217	2.248	1.996
no. of unique rflns, R_{int}	8621, 0.0957	9632, 0.0850	8365, 0.0907	6734, 0.1217
goodness of fit	1.052	0.918	1.063	0.735
final R indices $[I > 2\sigma(I)]$: R_1, wR_2	0.0348, 0.0855	0.0568, 0.1395	0.0362, 0.0936	0.0543, 0.0761
R indices (all data): R_1, wR_2	0.0475, 0.0910	0.0897, 0.1573	0.0418, 0.0969	0.2129, 0.1022

1.61 ($OC(\mathbf{CH_3})_3$, br, 36H), 6.69 (*meta*-C_5H_5N, m, 4H), 6.98 (*para*-C_5H_5N, m, 2H), 8.68 (*ortho*-C_5H_5N, br, 4H). ^{13}C NMR (C_6D_6, 25 °C): δ 34.5 ($OC(\mathbf{CH_3})_3$, br), 77.3 ($O\mathbf{C}(CH_3)_3$), 123.1 (*meta*-C_5H_5N), 135.2 (*para*-C_5H_5N), 150.0 (*ortho*-C_5H_5N). Anal. Calcd $CeO_4C_{26}H_{46}N_2$: C 52.86, H 7.85, N 4.74. Found: C 51.84, H 8.95, N 3.32.

Synthesis of $Ce_3O(O^tBu)_{10}$ (2). A 0.84 g portion (1.5 mmol) of $Ce(O^tBu)_4(THF)_2$ was dissolved in *n*-heptane and was stirred for 4 days at room temperature. All volatiles were evaporated under reduced pressure, and the product was obtained as a yellow powder in nearly quantitative yield (0.54 g, 95%). ^1H NMR (C_6D_6, 25 °C): δ 1.44 ($OC(\mathbf{CH_3})_3$, s, 27H), 1.45 ($OC(\mathbf{CH_3})_3$, s, 27H), 1.92 (μ_2-$OC(\mathbf{CH_3})_3$, s, 27H), 1.95 (μ_3-$OC(\mathbf{CH_3})_3$, s, 9H). ^{13}C NMR (C_6D_6, 25 °C): δ 33.9 ($OC(\mathbf{CH_3})_3$), 34.1 ($OC(\mathbf{CH_3})_3$), 34.8 (μ_2-$OC(\mathbf{CH_3})_3$), 35.2 (μ_3-$OC(\mathbf{CH_3})_3$), 74.8 (μ_3-$O\mathbf{C}(CH_3)_3$), 78.0 (μ_2-$O\mathbf{C}(CH_3)_3$), 83.0 ($O\mathbf{C}(CH_3)_3$), 83.6 ($O\mathbf{C}(CH_3)_3$). Anal. Calcd $Ce_3O_{11}C_{40}H_{90}$: C 41.15, H 7.77 Found: C 43.53, H 9.25. Deviations to higher carbon and hydrogen contents are caused by nonstoichiometric intercalated *n*-heptane molecules.

Synthesis of $KCe_2(O^tBu)_9$ (3). A solution of 1.35 g (12.0 mmol) of KO^tBu in 20 mL of THF was added to a solution of 1.01 g (1.8 mmol) of CAN in 25 mL of THF at room temperature and stirred for 2 h. The yellow solution was separated from the white precipitate by decantation, and all volatiles were removed under reduced pressure. The product was crystallized as yellow plates from a concentrated *n*-heptane solution (1.51 g, 86%). The^1H NMR (C_6D_6, 25 °C): δ 1.40 ($\mu_{2(Ce-K)}$-$OC(\mathbf{CH_3})_3$, s, 18H), 1.63 ($OC(\mathbf{CH_3})_3$, s, 36H), 1.73 (μ_3-$OC(\mathbf{CH_3})_3$, s, 18H), 1.90 ($\mu_{2(Ce-Ce)}$-$OC(\mathbf{CH_3})_3$, s, 9H). ^{13}C NMR (C_6D_6, 25 °C): δ 34.6 ($OC(\mathbf{CH_3})_3$), 34.9 ($\mu_{2(Ce-K)}$-$OC(\mathbf{CH_3})_3$), 35.6 ($\mu_{2(Ce-Ce)}$-$OC(\mathbf{CH_3})_3$), 35.7 (μ_3-$OC(\mathbf{CH_3})_3$), 75.0 (μ_3-$O\mathbf{C}(CH_3)_3$), 76.3 ($\mu_{2(Ce-Ce)}$-$O\mathbf{C}(CH_3)_3$), 77.3 ($\mu_{2(Ce-K)}$-$O\mathbf{C}(CH_3)_3$), 82.4 ($O\mathbf{C}(CH_3)_3$). Anal. Calcd $KCe2O_9C_{36}H_{81}$: C 44.24, H 8.35 Found: C 44.99, H 10.22.

Synthesis of $AlCe(O^tBu)_7$ (4). A 2.18 g portion (4.0 mmol) of CAN was dissolved in 30 mL of THF, and a solution of 2.69 g (24.0 mmol) of KO^tBu in 20 mL of THF was added. To the reaction mixture a solution of 0.99 g (2.0 mmol) of $[Al(O^tBu)_3]_2$ in 20 mL of THF was added; the mixture was stirred for 2 h at room temperature. All volatiles were evaporated under reduced pressure, and the product was extracted from the precipitated KNO_3 by washing the residue twice with two portions of 20 mL *n*-heptane. The solution was evaporated to dryness, and 1.85 g of the product was obtained by vacuum sublimation at 140 °C (10^{-2} mbar) as a bright yellow powder (68%). ^1H NMR (C_6D_6, 25 °C): δ 1.43 (Al-$OC(\mathbf{CH_3})_3$, s, 9H), 1.44

(Ce-OC(**CH**$_3$)$_3$, s, br, 27H), 1.57 (μ_2-OC(**CH**$_3$)$_3$, s, 27H). ^{13}C NMR (C$_6$D$_6$, 25 °C): δ 33.3 (Ce-OC(**C**H$_3$)$_3$, μ_2-OC(**C**H$_3$)$_3$, br), 34.7 (Al-OC(**C**H$_3$)$_3$), 68.7 (Al–O**C**(CH$_3$)$_3$), 71.3 (μ_2-O**C**(CH$_3$)$_3$), 83.7 (Ce–O**C**(CH$_3$)$_3$). ^{27}Al NMR (C$_6$D$_6$, 25 °C): δ 59 ($w_{1/2}$ = 1400 Hz). EI-MS (20 eV, 100 °C): *m/z* (intensity) 663 (5, [M −CH$_3$]$^+$), 605 (100, [M − OC$_4$H$_9$]$^+$), 589 (5, [M − OC$_4$H$_9$–CH$_4$]$^+$), 532 (5, [M − 2(OC$_4$H$_9$)]$^+$), 475 (5, [CeAlO(OC$_4$H$_9$)$_4$]$^+$). Anal. Calcd CeAlO$_7$C$_{28}$H$_{63}$: C 49.54, H 9.35. Found: C 49.12, H 6.96.

Synthesis of FeCe(O^{t}Bu)$_7$ (5). The synthetic procedure was similar to that described for **4**, starting from 1.34 g (2.4 mmol) of [Fe(O^{t}Bu)$_3$]$_2$, 2.63 g (4.8 mmol) of CAN, and 3.23 g (28.8 mmol) of KO^{t}Bu. A 2.12 g portion of the product was obtained as a yellow powder by vacuum sublimation at 150 °C (10^{-2} mbar) (62%). EI-MS (20 eV, 100 °C): *m/z* (intensity) 692 (7, [M −CH$_3$]$^+$), 634 (100, [M − OC$_4$H$_9$]$^+$), 561 (5, [M −2(OC$_4$H$_9$)]$^+$), 504 (9, [CeFeO(OC$_4$H$_9$)$_4$]$^+$). Anal. Calcd CeFeO$_7$C$_{28}$H$_{63}$: C 47.52, H 8.97. Found: C 48.02, H 6.84.

Synthesis of AlCe(O^{t}Bu)$_7$(py) (6). The product was obtained as a bright yellow powder in nearly quantitative yield (0.90 g, 99%) by dissolving 0.83 g (1.2 mmol) of AlCe(O^{t}Bu)$_7$ in dry pyridine. Crystals suitable for single crystal X-ray diffraction were grown from a concentrated *n*-heptane solution at −18 °C. ^{1}H NMR (C$_6$D$_6$, 25 °C): δ 1.48 (Ce-OC(**CH**$_3$)$_3$, s, br, 27H), 1.62 (μ_2-OC(**CH**$_3$)$_3$ and Al OC(**CH**$_3$)$_3$, s, br, 36H), 6.82 (*meta*-C$_5$H$_5$N, dd, 2H), 7.00 (*para*-C$_5$H$_5$N, dd, 1H), 9.26 (*ortho*-C$_5$H$_5$N, br, 2H). ^{13}C NMR (C$_6$D$_6$, 25 °C): δ 33.6 (OC(**C**H$_3$)$_3$, br), 70.7 (μ_2-O**C**(CH$_3$)$_3$ and Al–O**C**(CH$_3$)$_3$), 82.8 (Ce–O**C**(CH$_3$)$_3$), 122.7 (*meta*-C$_5$H$_5$N), 136.5 (*para*-C$_5$H$_5$N), 151.1 (*ortho*-C$_5$H$_5$N). ^{27}Al NMR (C$_6$D$_6$, 25 °C): δ 47 ($w_{1/2}$ = 1200 Hz). Anal. Calcd CeAlO$_7$C$_{33}$H$_{68}$N: C 52.29, H 9.04, N 1.85. Found: C 52.94, H 10.30, N 0.83.

Synthesis of FeCe(O^{t}Bu)$_7$(py) (7). The reaction was carried out under similar conditions to that described for **6** starting from 1.86 g (2.6 mmol) of **5** which afforded the product as yellow powder in quantitative yield (2.07, 100%). Crystals were obtained from a concentrated *n*-heptane solution at −18 °C. Anal. Calcd CeFeO$_7$C$_{33}$H$_{68}$N: C 50.37, H 8.71, N 1.78. Found: C 50.24, H 10.61, N 0.62.

Synthesis of GeCe(O^{t}Bu)$_6$ (8). A 2.85 g portion (5.2 mmol) of CAN was dissolved in 30 mL of THF, and a solution of 3.05 g (31.2 mmol) of KO^{t}Bu in 20 mL of THF was added. To the reaction mixture a solution of 1.14 g (2.6 mmol) of [Ge(O^{t}Bu)$_2$]$_2$ in 25 mL of THF was added and stirred at room temperature for 2 h. The yellow solution was separated from the white precipitate by decantation. The reaction mixture was evaporated to dryness, and the crude product was purified by vacuum sublimation at 130 °C (10^{-2} mbar) (yellow powder, 2.21 g, 65%). ^{1}H NMR (C$_6$D$_6$, 25 °C): δ 1.47 (μ_2-OC(**CH**$_3$)$_3$, s, 27H), 1.49 (OC(**CH**$_3$)$_3$, s, 27H). ^{13}C NMR (C$_6$D$_6$, 25 °C): δ 32.9 (OC(**C**H$_3$)$_3$), 33.9 (μ_2-OC(**C**H$_3$)$_3$), 74.4 (μ_2-O**C**(CH$_3$)$_3$), 82.0 (O**C**(CH$_3$)$_3$). EI-MS (20 eV, 105 °C): *m/z* (intensity) 652 [M]$^+$ (18%), 579 [M − OC$_4$H$_9$]$^+$ (100%), 522 [M −2(OC$_4$H$_9$)]$^+$ (26%), 466 [CeGe(O)(OH)(OC$_4$H$_9$)$_3$] (5%), 449 [CeGe(O)(OC$_4$H$_9$)$_3$]$^+$ (15%), 59 [OC$_3$H$_6$]$^+$ (13%). Anal. Calcd CeGeO$_6$C$_{24}$H$_{54}$: C 44.25, H 8.36. Found: C 43.73, H 8.96.

Synthesis of SnCe(O^{t}Bu)$_6$ (9). The synthetic procedure was similar to that described for **8**, starting from 0.98 g (1.8 mmol) of [Sn(O^{t}Bu)$_2$]$_2$, 2.03 g (3.7 mmol) of CAN and 2.49 g (22.2 mmol) of KO^{t}Bu. The crude product was purified by vacuum sublimation at 150 °C (10^{-2} mbar) (yellow powder, 1.83 g, 71%). ^{1}H NMR (C$_6$D$_6$, 25 °C): δ 1.46 (μ_2-OC(**CH**$_3$)$_3$, s, 27H), 1.50 (OC(**CH**$_3$)$_3$, s, 27H). ^{13}C NMR (C$_6$D$_6$, 25 °C): δ 34.1 (OC(**C**H$_3$)$_3$), 34.3 (μ_2-OC(**C**H$_3$)$_3$, $^3J(^{13}\mathrm{C},^{119}\mathrm{Sn})$ = 26 Hz), 73.7 (μ_2-O**C**(CH$_3$)$_3$), 81.7 (O**C**(CH$_3$)$_3$). ^{119}Sn NMR (C$_6$D$_6$, 25 °C): δ −249. EI-MS (20 eV, 110 °C): *m/z* (intensity) 698 [M]$^+$ (5%), 625 [M − OC$_4$H$_9$]$^+$ (100%), 552 [M − 2(OC$_4$H$_9$)]$^+$ (6%), 495 [CeSn(OH)(OC$_4$H$_9$)$_3$]$^+$ (7%), 59 [OC$_3$H$_6$]$^+$ (12%). Anal. Calcd CeSnO$_6$C$_{24}$H$_{54}$: C 41.33, H 7.80. Found: C 40.25, H 8.21.

Synthesis of PbCe(O^{t}Bu)$_6$ (10). The synthetic procedure was similar to that described for **8**, starting from 1.14 g (1.1 mmol) of [Pb(O^{t}Bu)$_2$]$_3$, 1.75 g (3.2 mmol) of CAN, and 2.15 g (19.2 mmol) of KO^{t}Bu. The crude product was purified by vacuum sublimation at 150 °C (10^{-2} mbar) (yellow powder, 1.64 g, 65%). ^{1}H NMR (C$_6$D$_6$, 25 °C): δ 1.42 (μ_2-OC(**CH**$_3$)$_3$, s, 27H), 1.57 (OC(**CH**$_3$)$_3$, s, 27H). ^{13}C NMR (C$_6$D$_6$, 25 °C): δ 34.3 (OC(**C**H$_3$)$_3$), 35.2 (μ_2-OC(**C**H$_3$)$_3$, $^3J(^{13}\mathrm{C},^{207}\mathrm{Pb})$ = 25 Hz), 72.8 (μ_2-O**C**(CH$_3$)$_3$, $^2J(^{13}\mathrm{C},^{207}\mathrm{Pb})$ = 5 Hz), 80.9 (O**C**(CH$_3$)$_3$). ^{207}Pb NMR (C$_6$D$_6$, 25 °C): δ 1356. EI-MS (20 eV, 120 °C): *m/z* (intensity) 713 [M − O$_4$H$_9$]$^+$ (100%), 640 [M − 2(OC$_4$H$_9$)]$^+$ (7%), 583 [CePb(O)(OC$_4$H$_9$)$_3$]$^+$ (5%), 59 [OC$_3$H$_6$]$^+$ (52%). Anal. Calcd CePbO$_6$C$_{24}$H$_{54}$: C 36.67, H 6.92. Found: C 35.77, H 7.25.

Synthesis of (CO)$_5$MoGe(μ_2-O^{t}Bu)$_3$Ce(O^{t}Bu)$_3$ (11). A 0.63 g portion (1.0 mmol) of GeCe(O^{t}Bu)$_6$ and 0.26 g (1.0 mmol) of Mo(CO)$_6$ were dissolved in 20 mL of toluene and heated under reflux for 3 days. The reaction mixture was evaporated to dryness a yellow solution was extracted by 20 mL of *n*-heptane. From a concentrated solution a mixture of yellow crystals of the product and **8** were obtained by crystallization (0.34 g). ^{1}H NMR (C$_6$D$_6$, 25 °C): δ 1.37 (OC(**CH**$_3$)$_3$, s, 27H). 1.57 (μ_2-OC(**CH**$_3$)$_3$, s, 27H). ^{13}C NMR (C$_6$D$_6$, 25 °C): δ 33.6 (μ_2-OC(**C**H$_3$)$_3$), 34.8 (OC(**C**H$_3$)$_3$), 76.2 (μ_2-O**C**(CH$_3$)$_3$), 83.8 (O**C**(CH$_3$)$_3$), 206.8 (**C**O$_{\mathrm{eq}}$), 210.0 (**C**O$_{\mathrm{ax}}$). IR (KBr): ν_{CO} 1930 (vs), 1967 (sh), 2073 (m).

Synthesis of (CO)$_5$MoSn(μ_2-O^{t}Bu)$_3$Ce(O^{t}Bu)$_3$ (12). The synthetic procedure was similar to that described for **11**, starting from 0.82 g (1.2 mmol) of SnCe(O^{t}Bu)$_6$ and 0.31 g (1.2 mmol) of Mo(CO)$_6$. From a concentrated *n*-heptane solution a mixture of yellow crystals of the product and **9** were obtained by crystallization (0.46 g).^{1}H NMR (C$_6$D$_6$, 25 °C): δ 1.42 (OC(**CH**$_3$)$_3$, s, 27H), 1.52 (μ_2-OC(**CH**$_3$)$_3$, s, 27H). ^{13}C NMR (C$_6$D$_6$, 25 °C): δ 33.5 (μ_2-OC(**C**H$_3$)$_3$), 34.8 (OC(**C**H$_3$)$_3$), 75.2 (μ_2-O**C**(CH$_3$)$_3$), 83.2 (O**C**(CH$_3$)$_3$), 206.2 (**C**O$_{\mathrm{eq}}$), 209.7 (**C**O$_{\mathrm{ax}}$). ^{119}Sn NMR (C$_6$D$_6$, 25 °C): δ −16. IR (KBr): ν_{CO} 1942 (vs), 1976 (sh), 2077 (m).

ASSOCIATED CONTENT

Supporting Information

Molecular structures and selected bond lengths and angles of **5**, **7**, **12**. X-ray crystallographic data files in CIF format. This material is available free of charge via the Internet at http://pubs.acs.org.

AUTHOR INFORMATION

Corresponding Author

*E-mail: sanjay.mathur@uni-koeln.de..

Notes

The authors declare no competing financial interest.

ACKNOWLEDGMENTS

Authors are thankful to the University of Cologne and Korean Institute of Technology, Incheon (KITECH) for the financial assistance.

REFERENCES

(1) Trovarelli, A. *Catal. Rev.: Sci. Eng.* **1996**, *38*, 439−520.

(2) Yuan, Q.; Duan, H.-H.; Li, L.-L.; Sun, L.-D.; Zhang, Y.-W.; Yan, C.-H. *J. Colloid Interface Sci.* **2009**, *335*, 151−167.

(3) (a) Veith, M.; Mathur, S.; Mathur, C. *Polyhedron* **1998**, *17*, 1005−1034. (b) Mathur, S.; Veith, M.; Shen, H.; Hüfner, S.; Jilavi, M. H. *Chem. Mater.* **2002**, *14*, 568−582. (c) Bemm, U.; Norrestam, R.; Nygren, M.; Westin, G. *Inorg. Chem.* **1995**, *34*, 2367. (d) Moustiakimov, M.; Kritikos, M.; Westin, G. *Inorg. Chem.* **2005**, *44*, 1499. (e) Veith, M.; Mathur, S.; Huch, V. *J. Am. Chem. Soc.* **1996**, *118*, 903.

(4) (a) Hubert-Pfalzgraf, L. G. *Inorg. Chem. Commun.* **2003**, *6*, 102−120. (b) Veith, M.; Mathur, S.; Shen, H.; Lecerf, N.; Hüfner, S.; Jilavi, M. H. *Chem. Mater.* **2001**, *13*, 4041−4052. (c) Mathur, S.; Shen, H.; Rapalaviciute, R.; Kareiva, A.; Donia, N. *J. Mater. Chem.* **2004**, *14*, 1. (d) Mathur, S.; Veith, M.; Rapalaviciute, R.; Shen, H.; Goya, G. F.; Martins, W. L. F.; Berquo, T. S. *Chem. Mater.* **2004**, *16* (10), 1906.

(5) (a) Bradley, D. C.; Chatterjee, A. K.; Wardlaw, W. *J. Chem. Soc.* **1955**, 2260−2264. (b) Bradley, D. C.; Chatterjee, A. K.; Wardlaw, W.

J. Chem. Soc. **1956**, 3469−3472. (c) Bradley, D. C.; Chatterjee, A. K.; Wardlaw, W. *J. Chem. Soc.* **1957**, 2600−2604.

(6) Gradeff, P. F.; Schreiber, F. G.; Brooks, K. C.; Sievers, R. E. *Inorg. Chem.* **1985**, *24*, 1110−1111.

(7) Evans, W. J.; Deming, T. J.; Olofson, J. M.; Ziller, J. W. *Inorg. Chem.* **1989**, *28*, 4027−4034.

(8) Suh, S.; Guan, J.; Mîinea, L. A.; Lehn, J.-S. M.; Hoffman, D. M. *Chem. Mater.* **2004**, *16*, 1667−1673.

(9) Toledano, P. P.; Ribot, F.; Sanchez, C. *Acta Crystallogr., Sect. C: Cryst. Struct. Commun.* **1990**, *C46*, 1419−1422.

(10) Sirio, C.; Hubert-Pfalzgraf, L. G.; Bois, C. *Polyhedron* **1997**, *16*, 1129−1136.

(11) Sen, A.; Stecher, H. A.; Rheingold, A. L. *Inorg. Chem.* **1992**, *31*, 473−479.

(12) Gun'ko, Y. K.; Elliott, S. D.; Hitchcock, P. B.; Lappert, M. F. *J. Chem. Soc., Dalton Trans.* **2002**, 1852−1856.

(13) Arnold, P. L.; Casely, I. J.; Zlatogorsky, S.; Wilson, C. *Helv. Chim. Acta* **2009**, *92*, 2291−2303.

(14) Yunlu, K.; Gradeff, P. S.; Edelstein, N.; Kot, W.; Shalimoff, G.; Streib, W. E.; Vaartstra, B. A.; Caulton, K. G. *Inorg. Chem.* **1991**, *30*, 2317−2321.

(15) (a) Wrench, J. S.; Black, K.; Aspinall, H. C.; Jones, A. C.; Bacsa, J.; Chalker, P. R.; King, P. J.; Werner, M.; Davies, H. O.; Heys, P. N. *Chem. Vap. Deposition* **2009**, *15*, 259−261. (b) Aspinall, H. C.; Basca, J.; Jones, A. C.; Wrench, J. S.; Black, K.; Chalker, P. R.; King, P. J.; Marshall, P.; Werner, M.; Davies, H. O.; Odedra, R. *Inorg. Chem.* **2011**, *50*, 11644−11652. (c) Hubert-Pfalzgraf, L. G.; El Khokh, N. *Polyhedron* **1992**, *11*, 59−63.

(16) (a) Hubert-Pfalzgraf, L. G.; Abada, V.; Vaissermann, J. *J. Chem. Soc., Dalton Trans.* **1998**, 3437−3441. (b) Daniele, S.; Hubert-Pfalzgraf, L. G.; Perrin, M. *Polyhedron* **2002**, *21*, 1985−1990.

(17) Kim, H.; Kim, Y. T.; Chae, H. K. *J. Sol-Gel Sci. Technol.* **2005**, *33*, 75−80.

(18) Hubert-Pfalzgraf, L. G.; Abada, V.; Vaissermann, J. *Polyhedron* **1999**, *18*, 3497−3504.

(19) Hubert-Pfalzgraf, L. G.; Sirio, C.; Bois, C. *Polyhedron* **1998**, *17*, 821−830.

(20) Broderick, E. M.; Thuy-Boun, P. S.; Guo, N.; Vogel, C. S.; Sutter, J.; Miller, J. T.; Meyer, K.; Diaconescu, P. L. *Inorg. Chem.* **2011**, *50*, 2870−2877.

(21) Lorber, C.; Choukroun, R.; Vendier, L. *Organometallics* **2008**, *27*, 5017−5024.

(22) Clark, D. L.; Watkin, J. G. *Inorg. Chem.* **1993**, *32*, 1766−1772.

(23) Van der Sluys, W. G.; Sattelberger, A. P.; McElfresh, M. W. *Polyhedron* **1990**, *9*, 1843−1848.

(24) Cotton, F. A.; Marler, D. O.; Schwotzer, W. *Inorg. Chim. Acta* **1984**, *95*, 207−209.

(25) Starikova, Z. A.; Turevskaya, E. P.; Kozlova, N. I.; Turova, N. Ya.; Berdyev, D. V.; Yanovsky, A. I. *Polyhedron* **1999**, *18*, 941−947.

(26) Poncelet, O.; Sartain, W. J.; Hubert-Pfalzgraf, L. G.; Folting, K.; Caulton, K. B. *Inorg. Chem.* **1989**, *28*, 263−267.

(27) Cotton, F. A.; Marler, D. O.; Schwotzer, W. *Inorg. Chem.* **1984**, *23*, 4211−4215.

(28) Teff, D. J.; Huffman, J. C.; Caulton, K. G. *Inorg. Chem.* **1994**, *33*, 6289−6292.

(29) Veith, M.; Weidner, S.; Kunze, K.; Käfer, D.; Hans, J.; Huch, V. *Coord. Chem. Rev.* **1994**, *137*, 297−322.

(30) Teff, D. J.; Huffman, J. C.; Caulton, K. G. *Inorg. Chem.* **1996**, *35*, 2981−2987.

(31) Fortier, S.; Wu, G.; Hayton, T. W. *Inorg. Chem.* **2008**, *47*, 4752−4761.

(32) Mathur, S. Chemical Synthesis of Nanostructured Materials. Habilitation Thesis, Saarland University, Saarbrücken, Germany, 2004.

(33) (a) Berger, E.; Westin, G. *J. Sol-Gel Sci. Technol.* **2010**, *53*, 681−688. (b) Veith, M.; Yu, E.-C.; Huch, V. *Chem.—Eur. J.* **1995**, *1*, 26−32.

(34) Cordero, B.; Gómez, V.; Platero-Prats, A. E.; Revés, M.; Echeverría, J.; Cremades, E.; Barragán, F.; Alvarez, S. *Dalton Trans.* **2008**, 2832−2838.

(35) Njua, E. Y.; Steiner, A.; Stahl, L. *Inorg. Chem.* **2010**, *49*, 2163−2172.

(36) (a) Garg, G.; Singh, A.; Mehrotra, R. C. *Indian J. Chem., Sect. A: Inorg., Bio-inorg., Phys., Theor. Anal. Chem.* **1991**, *30*, 866−871. (b) Garg, G.; Dubey, R. K.; Singh, A.; Mehrotra, R. C. *Polyhedron* **1991**, *10*, 1733−1739. (c) Dubey, R. K.; Singh, A.; Mehrotra, R. C. *Indian J. Chem., Sect. A: Inorg., Bio-inorg., Phys., Theor. Anal. Chem.* **1992**, *31*, 156−159.

(37) Spandl, J.; Kusserow, M.; Brüdgam, I. *Z. Anorg. Allg. Chem.* **2003**, *629*, 968−974.

(38) Sparkes, H. A.; Raithby, P. R.; Clot, E.; Shields, G. P.; Chisholm, J. A.; Allen, F. H. *CrystEngComm* **2006**, *8*, 563−570.

(39) Veith, M.; Kunze, K. *Angew. Chem.* **1991**, *103*, 92−94.

(40) Veith, M.; Mathur, C.; Huch, V. *Phosphorus, Sulfur Silicon Relat. Elem.* **1997**, *124*, 489−492.

(41) Synthesis according to method 1: Kříž, O.; Čásenský, B.; Lyčka, A.; Fusek, J.; Heřmánek, S. *J. Magn. Reson.* **1984**, *60*, 375−381.

(42) Veith, M.; Hans, J.; Stahl, L.; May, P.; Huch, V.; Sebald, A. *Z. Naturforsch., B: Chem. Sci.* **1991**, *16*, 403−424.

(43) Fjeldberg, T.; Hitchcock, P. B.; Lappert, M. F.; Smith, S. J.; Thorne, A. J. *J. Chem. Soc., Chem. Commun.* **1985**, 939−941.

(44) *X-Area 1.16*; Stoe & Cie GmbH: Darmstadt, Germany, 2003.

(45) Farrugia, L. J. *J. Appl. Crystallogr.* **1999**, *32*, 837−838.

(46) Altomare, A.; Cascarano, G.; Giacovazzo, C.; Guagliardi, A. *J. Appl. Crystallogr.* **1993**, *26*, 343−350.

(47) Sheldrick, G. M. *SHELXL-97, Programs for Crystal Structure Analysis*; University of Göttingen: Göttingen, Germany, 1997.